Heliyon 9 (2023) e21333

Contents lists available at ScienceDirect

Heliyon

journal homepage: www.cell.com/heliyon

FOXD1 expression-based prognostic model for uveal melanoma

Yang Luo [a], Renhao Ni [a], Xiaojun Jin [a], Peipei Feng [b], Chenyi Dai [a], Lingjing Jiang [a], Pingping Chen [c], Lu Yang [d,**], Yabin Zhu [a,*]

[a] *Health Science Center, Ningbo University, Ningbo, 315211, China*
[b] *Ningbo Institute of Innovation for Combined Medicine and Engineering, Ningbo Medical Centre Lihuili Hospital, Ningbo, 315000, China*
[c] *Ningbo Eye Hospital, Ningbo, 315042, China*
[d] *The First Affiliated Hospital of Ningbo University, Ningbo, 315010, China*

ARTICLE INFO

Keywords:
FOXD1
Uveal melanoma
Patient survival
Treatment sensitivity
Prognostic model

ABSTRACT

FOXD1, a new member of the *FOX* transcription factor family, serves as a mediator and biomarker for cell reprogramming. But its contribution to prognosis of uveal melanoma (UVM) is unclear. This study demonstrated that *FOXD1* might promote tumor growth and invasion, because *FOXD1* expression was negatively correlated with overall survival, progression-free survival, and disease-specific survival in UVM patients. This conjecture was verified in cell culture with human uveal melanoma cell line (MUM2B) as model cells. Additionally, the biological mechanisms of *FOXD1* based on *FOXD1*-related genomic spectrum, molecular pathways, tumor microenvironment, and drug treatment sensitivity were examined using The Cancer Genome Atlas (TCGA) database, aiming to reasonably explain why *FOXD1* leads to poor prognosis of UVM. On these bases, a novel tumor prognostic model was established using the *FOXD1*-related immunomodulators *TMEM173*, *TNFRSF4*, *TNFSF13*, and *ULBP1*, which will enable the stratification of disease seriousness and clinical treatment for patients.

1. Introduction

The annual incidence rate of uveal melanoma (UVM), which is a malignant tumor involving iris, ciliary body, and choroid of eyes, is approximately 5.1 cases per million individuals [1]. The commonly used clinical treatment modalities for UVM include laser therapy, radiotherapy, and ophthalmectomy [2]. These conventional treatments achieve local tumor control. However, approximately 50 % of patients with UVM die within 10 years of diagnosis owing to metastasis [3].

The prognosis of patients with UVM is closely correlated with somatic mutation [4], tumor microenvironment and drug sensitivity of patients. For example, deletion of *BAP1* promotes the metastatic behavior of UVM. The mutation rate of *BAP1* reached 84 % in the metastatic UVM [5]. Other studies have shown that deletion of *BAP1* caused melanocytes to become a dedifferentiated stem cell like state, which may lead to the establishment of a premetastatic condition [6,7]. The interaction between the tumor cells and the peripheral cells existing in tumor microenvironment perhaps influences the development of tumors [8]. The infiltration of T cells and macrophages in tumor microenvironment may lead to poor prognosis of UVM patients [9]. Besides, different patients with UVM exhibit differential sensitivity to the same drug and consequently exhibit differential prognoses. Of eight patients with UVM treated

* Corresponding author.
** Corresponding author.
E-mail addresses: yanglu@nbu.edu.cn (L. Yang), zhuyabin@nbu.edu.cn (Y. Zhu).

https://doi.org/10.1016/j.heliyon.2023.e21333
Received 30 March 2023; Received in revised form 17 October 2023; Accepted 19 October 2023
Available online 23 October 2023

with pembrolizumab, one exhibited complete response, two exhibited partial response, one exhibited stable disease, and four exhibited rapid progression [10]. Therefore, the genome spectrum, tumor microenvironment, and drug sensitivity of patients must be analyzed to determine the prognosis of UVM.

FOXD1, a new member of the *FOX* transcription factor family [11], is locating at chromosome 5q12-q13 in humans, expressing in various tissues and cells, such as testis, kidney, central nervous system (optic chiasma, retina, pituitary), and serves as a mediator and indicator in cell reprogramming [12,13]. Recently, researchers have reported that *FOXD1* may cause the progression of some tumors like head and neck cancer, gastric cancer, oral squamous carcinoma, lung cancer, colorectal cancer and kidney cancer [14–19]. However, the function of *FOXD1* in UVM has not been elucidated so far.

This study demonstrated that the high expression of *FOXD1*decreased the survival rate of UVM patients. In addition, *FOXD1* knockdown weakened the proliferation and migration ability of UVM cells *in vitro*. This information suggests that *FOXD1* may cause poor prognosis of UVM patients. To further understand the potential role of *FOXD1* in UVM, *FOXD1*-related genomic spectrum, molecular pathways, tumor microenvironment, and drug sensitivity were analyzed. Finally, a novel tumor prognostic model was established using the *FOXD1*-related immunomodulators. We believe our prognostic model may help provide aid in the stratification of disease severity and the effective clinical treatment of patients.

2. Methods

2.1. Data sources

The mRNA sequencing data of patients with UVM (FPKM format, level 3 data), single-nucleotide variation data (Version: Masked Somatic Mutation) and clinical data (gender, survival time, and TNM stages (BCR XML format)) were obtained from the TCGA database (https://portal.gdc.cancer.gov/, Date of visit: January 22, 2022). The mRNA sequencing data were obtained from tumor tissues.

2.2. Correlation of FOXD1 with patient survival

The correlation of *FOXD1* with UVM patients' survival from TCGA database was analyzed using R language software. Referring to the middle expression level of *FOXD1*, 80 patients were separated into high-*FOXD1* and low-*FOXD1* expression groups. Overall survival (OS), progression free survival (PFS) and disease specific survival (DSS) of two groups were compared using R "Survival" package.

2.3. Analysis of single-nucleotide mutation

Single-nucleotide mutation data in patients from high-*FOXD1* and low-*FOXD1* expression groups were visualized by R "maftools" package, and the top 20 genes with the highest mutation frequency in the two groups were plotted, respectively.

2.4. Differential gene expression (DEG) analysis

DEGs between high-*FOXD1* and low-*FOXD1* expression groups were screened out via the R "limma" package in view of the following criteria: $|\log_2 \text{fold-change (FC)}| > 1$; $p < 0.05$. The criteria for correlation patterns between DEGs and *FOXD1* were as follows: when $\log_2 FC > 1$ and $p < 0.05$, positive correlation; when $\log_2 FC < -1$ and $p < 0.05$, negative correlation.

2.5. Functional enrichment analysis of genes

The "Limma", "org.hs.eg.db", "clusterProfiler", and "enrichPlot" packages in R were used to perform Gene ontology (GO) and Kyoto Encyclopedia of Genes and Genomes (KEGG) enrichment analysis to explore the biological functions of *FOXD1* related genes. The potential pathways of the highly enriched genes in both groups were subjected to gene set enrichment analysis (GSEA). The reference gene was set as follows: "H.all.v7.5.1. Symbols.Gmt". The criteria for determining the significantly enriched pathways were as follows: normalized enrichment score >1; nominal $p < 0.05$; false discovery rate (FDR) < 0.25.

2.6. Correlation of FOXD1 with microsatellite instability (MSI)

The correlation between MSI and *FOXD1* was drawn using R "limma", "ggplot2", "ggExtra", "ggpubr" packages and examined using the Spearman correlation test.

2.7. Correlation of FOXD1 with immune infiltrating cells

The correlation of *FOXD1* with the infiltration level of 22 immune cell types (including dendritic cells, monocytes, natural killer cells, plasma cells, T cells, and B cells) was determined via CIBERSORT algorithm (https://cibersort.stanford.edu/). In this study, the correlation was considered significant at $p < 0.05$. The correlation of *FOXD1* with the proportion of immune infiltrating cells was tested by using Spearman's correlation test. Single-sample GSEA (ssGSEA) was used to detect the activities of 13 immune-related pathways and infiltration scores of 16 immune cells inhigh-*FOXD1* expression and low-*FOXD1*expression groups with the R "GSVA" package.

2.8. Immune checkpoint expression and drug sensitivity

The box diagrams of immune checkpoint expression levels in high-*FOXD1* expression and low-*FOXD1* expression groups were drawn via R "reshape2", "ggplot2" and "ggpubr". The effectiveness of immunotherapy for UVM patients was evaluated via the tumor immune dysfunction and exclusion (TIDE) score, which was obtained from the TIDE online website (http://tide.dfci.harvard.edu/). The responses of the patients in two groups to chemotherapeutic and immunotherapeutic drugs were examined using the R "pRRophetic" package and the Genomics of Drug Sensitivity in Cancer web tool (https://www.cancerrxgene.org/).

2.9. Construction and verification of a risk-score model

FOXD1 related immune regulatory genes were excavated from TISIDB online database (http://cis.hku.hk/TISIDB/). Immunoinhibitors and immuno-stimulants significantly correlated with *FOXD1* were screened out using spearman correlation test ($p < 0.05$). The data from GSE84976 dataset in GEO database was used as validation queue. The batch difference in data of the two queues was eliminated using the "combat" method. Univariate Cox regression analysis was used to screen the OS-related immune regulatory genes in UVM patients. The "LASSO" method was used to remove redundant genes and build a prognosis model. Risk-score was calculated using the following formula: Risk-score = coefficient of gene A × expression level of gene A + coefficient of gene B × expression level of gene B + … …+ coefficient of gene N × expression level of gene N. UVM patients were separated into high-risk and low-risk groups according to the best risk-score cutoff. The difference in OS between the two groups was analyzed using R "Survival" package. The accuracy of the predictive model for predicting OS in patients with UVM was evaluated via ROC curves.

2.10. Construction and evaluation of clinical nomogram

The clinical variables, risk-score, gender and TNM stage, were integrated and evaluated via univariate and multivariate Cox regression analyses to set up a novel risk-score model. Additionally, a nomogram was constructed with these variables using the R "rms" package to quantitatively predict the prognosis in UVM patients. The accuracy of this nomogram in predicting 1-, 3- and 5-years OS in patients with UVM was assessed using ROC curve. The deviation between the predicted value and the actual probability of occurrence was shown by a calibration curve, which was drawn via the R "bootstrap" package.

2.11. Construction of MUM2B cell line with FOXD1 knockdown

The human UVM cell line (MUM2B (invasive)) was obtained from FuHeng Biotechnology Co., Ltd. (Shanghai, China). MUM2B cells were cultured in Roswell Park Memorial Institute-1640 medium supplemented with 10 % fetal bovine serum (FBS). The lentivirus harboring short-interfering RNA (si-RNA) against *FOXD1* (si-*FOXD1*) was obtained from Tsingke Biotechnology Co., Ltd (Beijing, China). The cells were transfected with lentivirus (multiplicity of infection = 10). The recombinant cells were screened with 0.75 μg/mL puromycin for 3 days and maintained in the presence of 0.2 μg/mL puromycin. Cells transfected with the lentivirus encoding negative control (NC) siRNA (si-NC) served as the control group.

The mRNA and protein levels of *FOXD1* were examined using quantitative real-time polymerase chain reaction (qRT-PCR) and western blotting, respectively. RNA was extracted by RNA Extraction Reagent (RNAiso Plus, TAKARA) and was transcribed into cDNA using the HiFiScript cDNA Synthesis Kit (CWBIO, China). qRT-PCR reaction was performed by Magic SYBR Mixture (CWBIO, China). The related mRNA expression was obtained using the $2^{-\Delta\Delta CT}$ method. Primer sequences of *FOXD1* and *β-actin* were listed in Supplementary Table S1. The total proteins of cells were extracted, followed by protein separation on sodium dodecyl sulfate gels (40μg/lane). After separation, the proteins were transferred to polyvinylidene fluoride (PVDF) membrane and sealed with a blocking solution. The protein on PVDF membrane was incubated overnight with the anti-*FOXD1* antibody (1:2000, PA5-35145, Thermo Fisher Scientific, USA) at 4 °C, and then incubated for 2h at room temperature with the goat anti-rabbit IgG (H + L) (1:5000, Proteintech, China). The enhanced chemiluminescence technology (Beyotime, China) was used to visualize the bands.

2.12. RNA sequencing and analysis

Total RNA was extracted from the si–NC–transfected MUM2B (MUM2BNC) and si-*FOXD1*-transfected (MUM2BKD) cells using the total RNA extraction reagent. RNA purity and quantification were examined using NanoDrop 2000 spectrophotometer (Thermo Scientific, USA). RNA integrity was assessed using the Agilent 2100Bioanalyzer (Agilent Technologies, Santa Clara, CA, USA). The libraries were constructed using VAHTS Universal V6 RNA-seq Library Prep Kit according to the manufacturer's instructions.

DEGs between MUM2BNC and MUM2BKD were screened out with screening criteria: $|\log_2(FC)| > 0.25$ and $p < 0.05$. The biological functions of these related genes were explored with GO and KEGG enrichment analysis.

2.13. Cell functional experiments in vitro and mRNA expression of related genes

Cell proliferation and clonogenic assays were carried out to evaluate the proliferation and clonogenicity, respectively, of MUM2BNC and MUM2BKD cells. Cells of MUM2BNC and MUM2BKD groups were inoculated on 96-well plates with the seeding density of 2000 cells/well and cultured for 24, 48, 72 and 96 h, respectively. The CCK-8 kit was used to detect the proliferation of cells. Clonogenic assay was carried out on 6-well plates, with the seeding density of 500 cells/well (MUM2BNC and MUM2BKD). The

cultures were incubated for 6 days, followed by staining with crystal violet aqueous solution (0.1 %, m/v).

Migration abilities of cells were tested by the Transwell chambers assays and scratch healing assay. Cells of MUM2BNC and MUM2BKD groups were inoculated in the upper chamber in 24-well culture plate, with the seeding density of 3×10^4 cells/well. The upper chamber comprised a serum-free medium (100 μL), while the lower chamber comprised a medium supplemented with 10 % FBS (500 μL). The cells were cultured for 15 h, stained with 0.1 % crystal violet aqueous solution, and imaged under a microscope. Scratch healing assay was carried out on 6-well plates. The cells were cultured until confluency, and the cell monolayer was scratched using a 200-μL pipette tip. The cells were cultured in the medium without serum. The scratched areas were observed and imaged at 0 and 24 h.

The mRNA expression of genes related to proliferation and migration was tested using qRT-PCR. Primer sequences of these genes were shown in Supplementary Table S1.

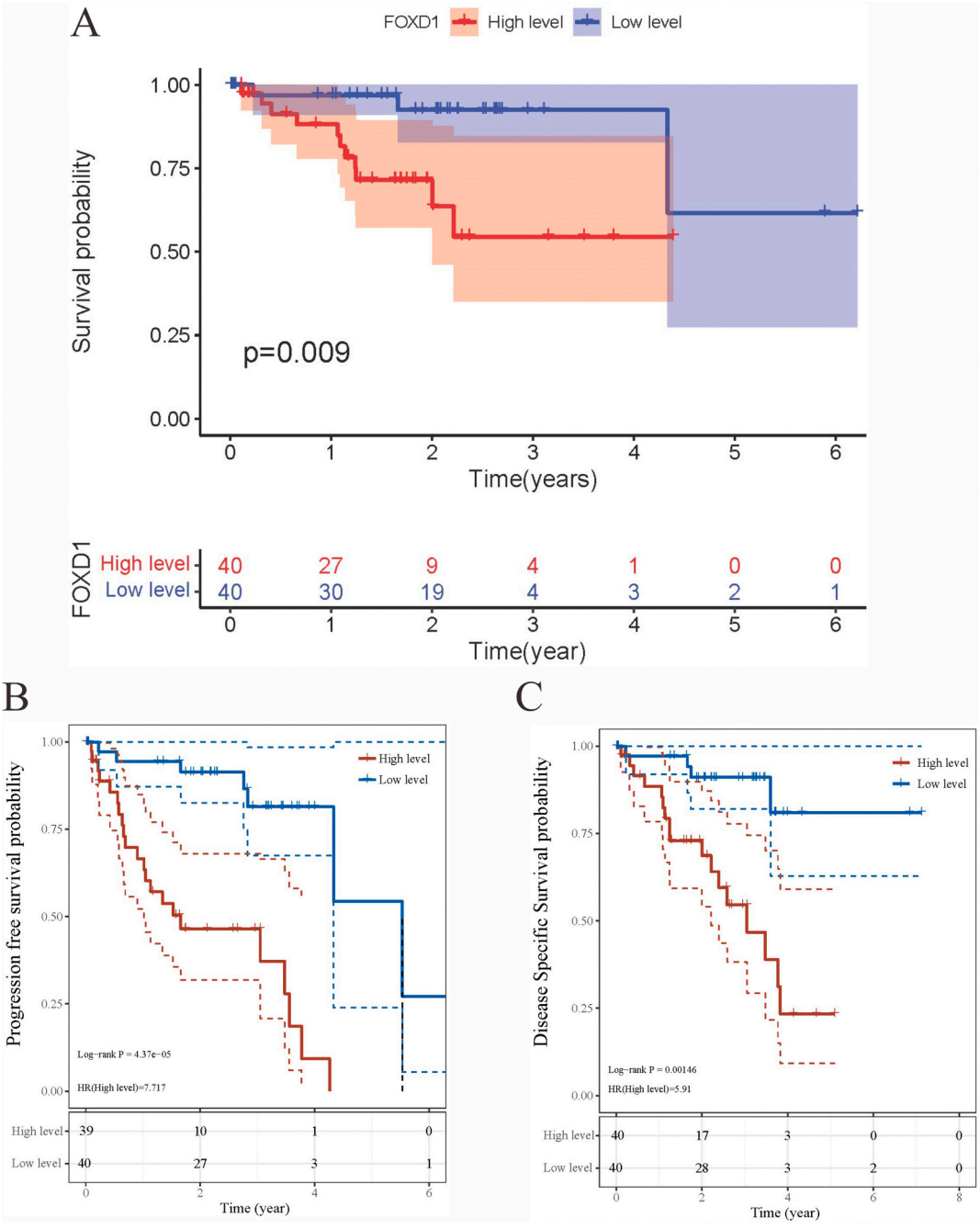

Fig. 1. Patient survival. **(A)** Overall survival; **(B)** Progression free survival; **(C)** Disease specific survival.

2.14. Statistical analysis

The analyses were performed using the R software (Version 4.0.3) and Prism software (GraphPad software Inc., version 9.3.1). The data are given as mean ± standard deviation (SD). Means were compared using the Student's t-test (for normally distributed variables) or the Wilcoxon rank-sum test (for non-normally distributed variables). $P < 0.05$ was considered differences as significance.

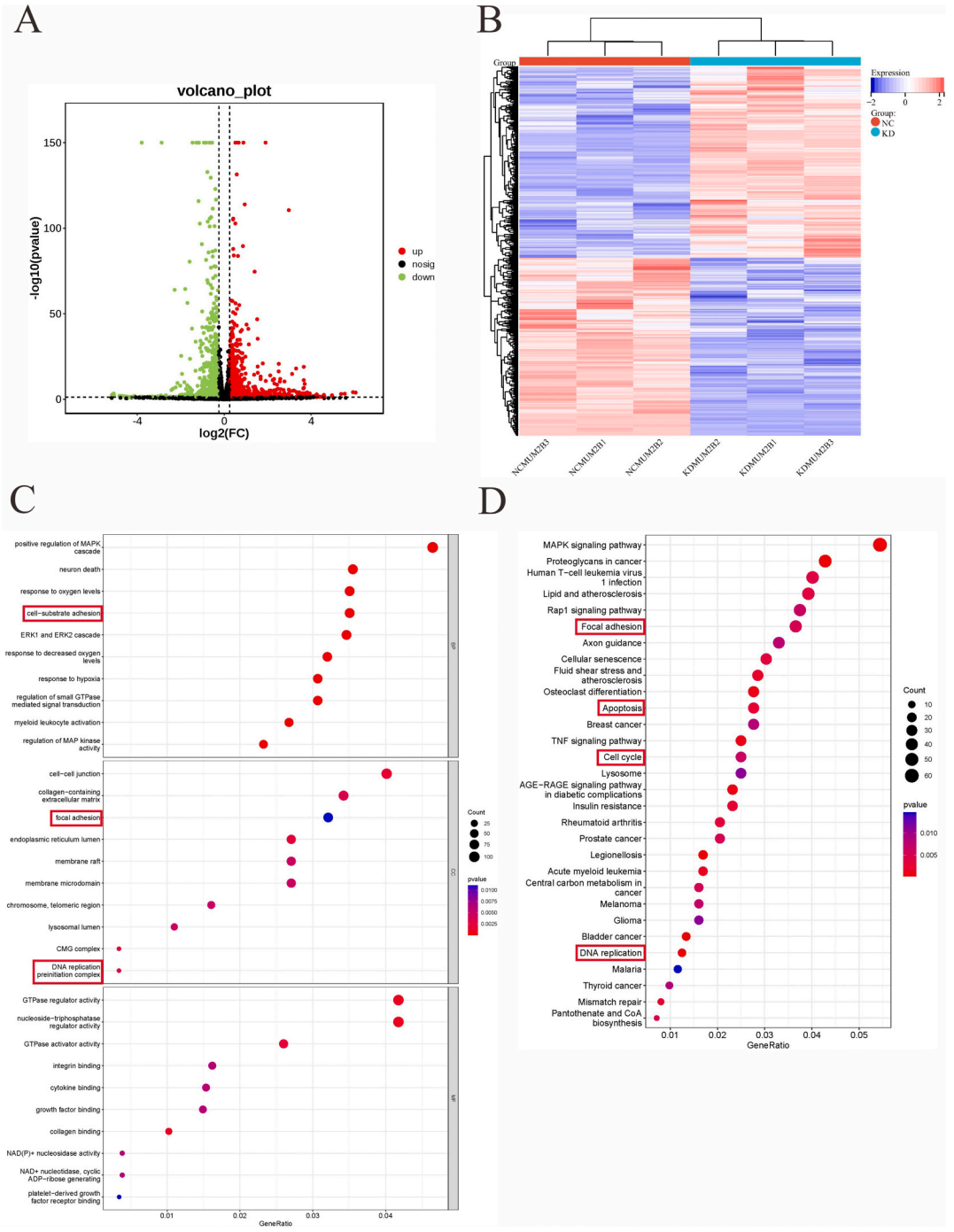

Fig. 2. RNA sequencing and data analysis. **(A, B)** Screening and display of differential genes; **(C)** GO enrichment analysis; **(D)** KEGG enrichment analysis.

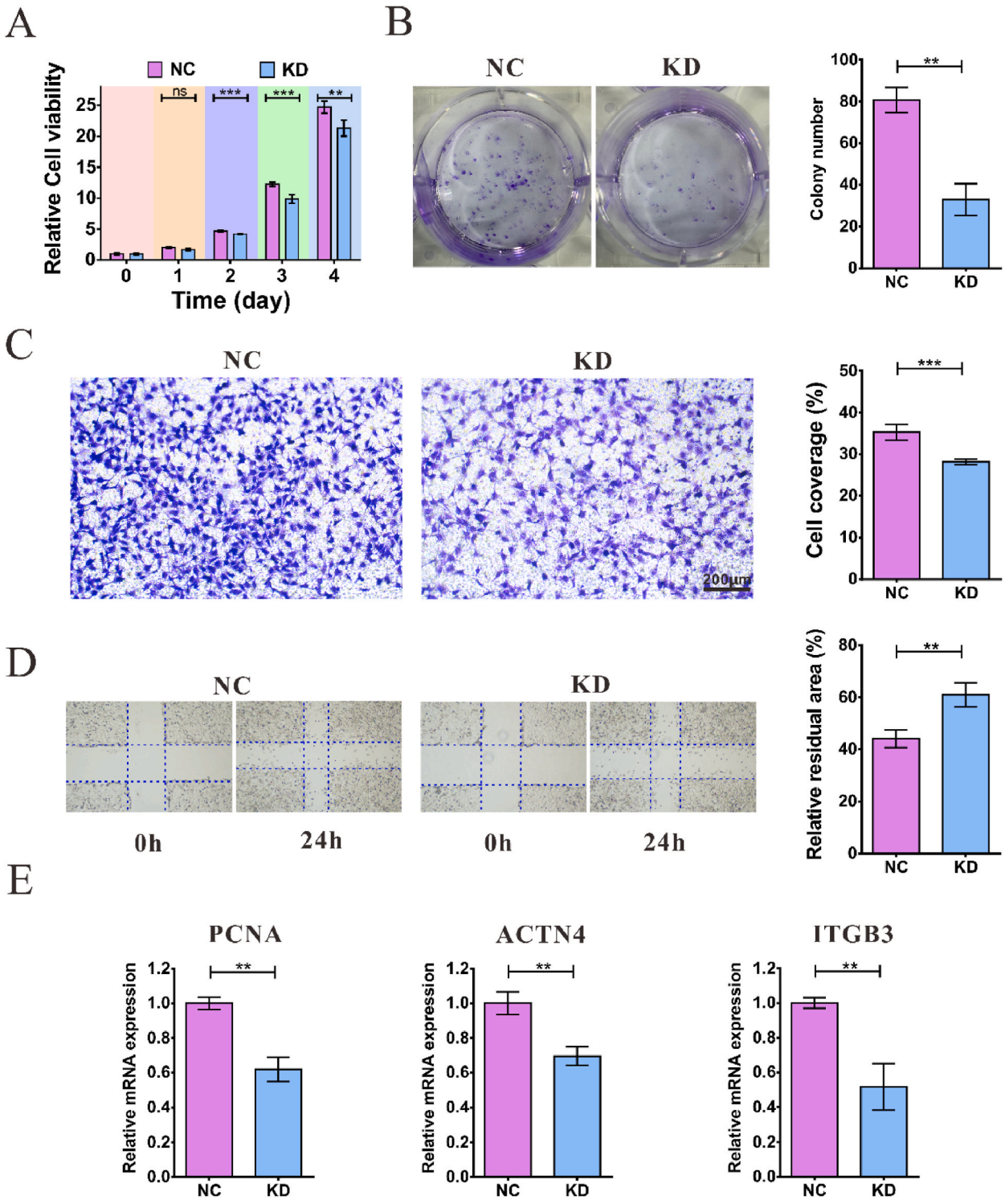

Fig. 3. Role of *FOXD1* on MUM2B cells. **(A)** The proliferation of si-negative control (NC)-transfected (MUM2BNC) and si-FOXD1-transfected (MUM2BKD) MUM2B cells; **(B)** Cell colonies formed after culturing for 6 days; **(C)** Migrating cells were imaged after culturing for 15 h; **(D)** Scratch healing assay with the MUM2BNC and MUM2BKD cells; **(E)** mRNA expression of genes related to proliferation and migration tested by qRT-PCR. $P < 0.05$ considered as statistically significance, $^{**}p < 0.01$, $^{***}p < 0.001$.

3. Results

3.1. Evaluation of the correlation between FOXD1 and UVM prognosis

3.1.1. FOXD1 reduces survival of UVM patients

As shown in Fig. 1, the survival rate of patients in the high-*FOXD1* expression and low-*FOXD1* expression groups decreased to various degrees over time. However, the OS (Fig. 1A), PFS (Fig. 1B), and DSS (Fig. 1C) of the low-*FOXD1* expression group were significantly higher than those of the high-*FOXD1* expression group. The survival of patients reflects the severity of the disease, which is closely related to the progression of UVM. Thus, we hypothesized that *FOXD1* is involved in the proliferation and migration of UVM cells.

3.1.2. FOXD1 involves in the proliferation and migration of UVM cells

FOXD1 knockdown MUM2B cells (MUM2BKD cells) were constructed, because both mRNA and protein expression of *FOXD1* were inhibited in MUM2BKD cells (Fig. S1). Next, MUM2BNC and MUM2BKD cells were subjected to RNA sequencing. The DEGs between cells of MUM2BNC and MUM2BKD groups were screened out to analyze the biological functions (Fig. 2A and B). GO analysis demonstrated that these genes are enriched in "cell-substrate adhesion", "focal adhesion" and "DNA replication preinitiation complex" (Fig. 2C). KEGG analysis suggests these genes are enriched in "focal adhesion", "apoptosis", "cell cycle", and "DNA replication" (Fig. 2D). These results indicated that *FOXD1* involved in the proliferation and migration of UVM cells. Further, we conducted cell experiments *in vitro* to clarify the specific role of *FOXD1* on UVM proliferation and migration.

3.1.3. FOXD1 knockdown reduces the proliferation and migration of UVM cells

The results of cell assays showed that the proliferation rate and clonogenicity of cells with *FOXD1* knockdown (MUM2BKD) reduced significantly during the culture interval, comparing with the control cells (MUM2BNC) (Fig. 3A and B). The migration ability of cells was tested by Transwell chamber assays after they were stained with crystal violet. The results exhibited that the color coverage area (proportional to cell number) of MUM2BKD group is less than that of MUM2BNC cells (Fig. 3C), which indicates that the number of migrating cells in MUM2BKD group is less than MUM2BNC group. That is, the migration ability of MUM2B cells with *FOXD1* knockdown becomes weak.

To further understand this function, the scratch healing assay was performed. The results showed that the speed to heal scratch in MUM2BKD cells was slower than that of MUM2BNC cells, indicating that cells migrated much slower after *FOXD1* gene was knockdown than the MUM2BNC cells (wild type, Fig. 3D). Thus, *FOXD1* does play an important role in maintaining the proliferation and migration capabilities for MUM2B cells.

mRNA levels of genes (*PCNA*, *ITGB3* and *ACTN4*) positively correlated with proliferation and migration capabilities was detected by qRT-PCR. *FOXD1* knockdown downregulated the mRNA levels of *PCNA*, *ITGB3*, and *ACTN4* in MUM2B cells (Fig. 3E). These results suggest that *FOXD1* may enhance the proliferation and migration of UVM cells by regulating the expression of these genes.

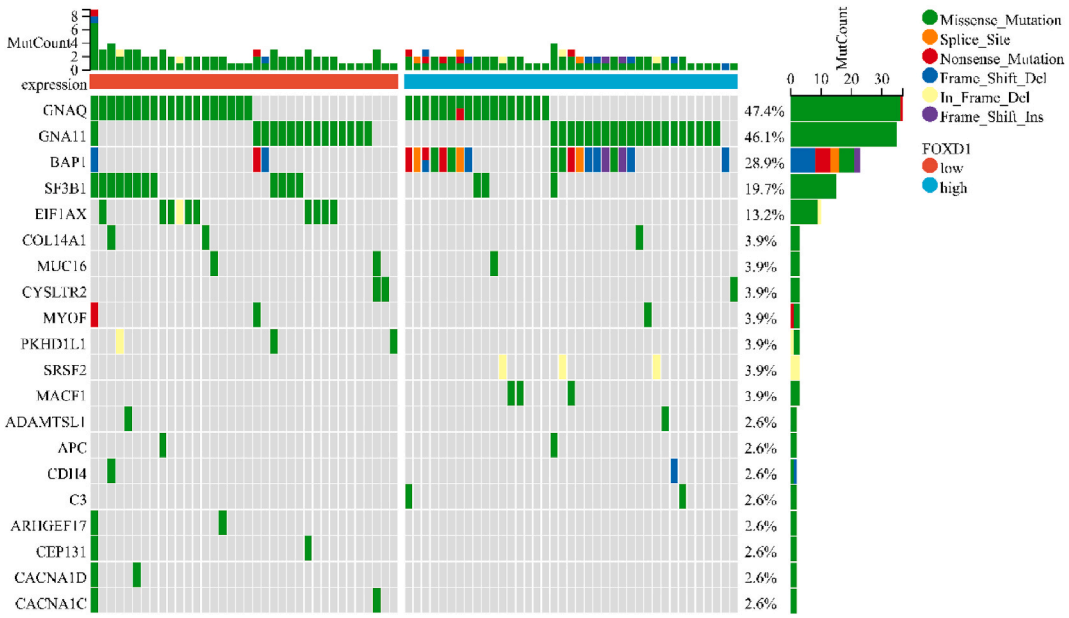

Fig. 4. Type and frequency of gene mutations in patients with high-*FOXD1* and low-*FOXD1* expression.

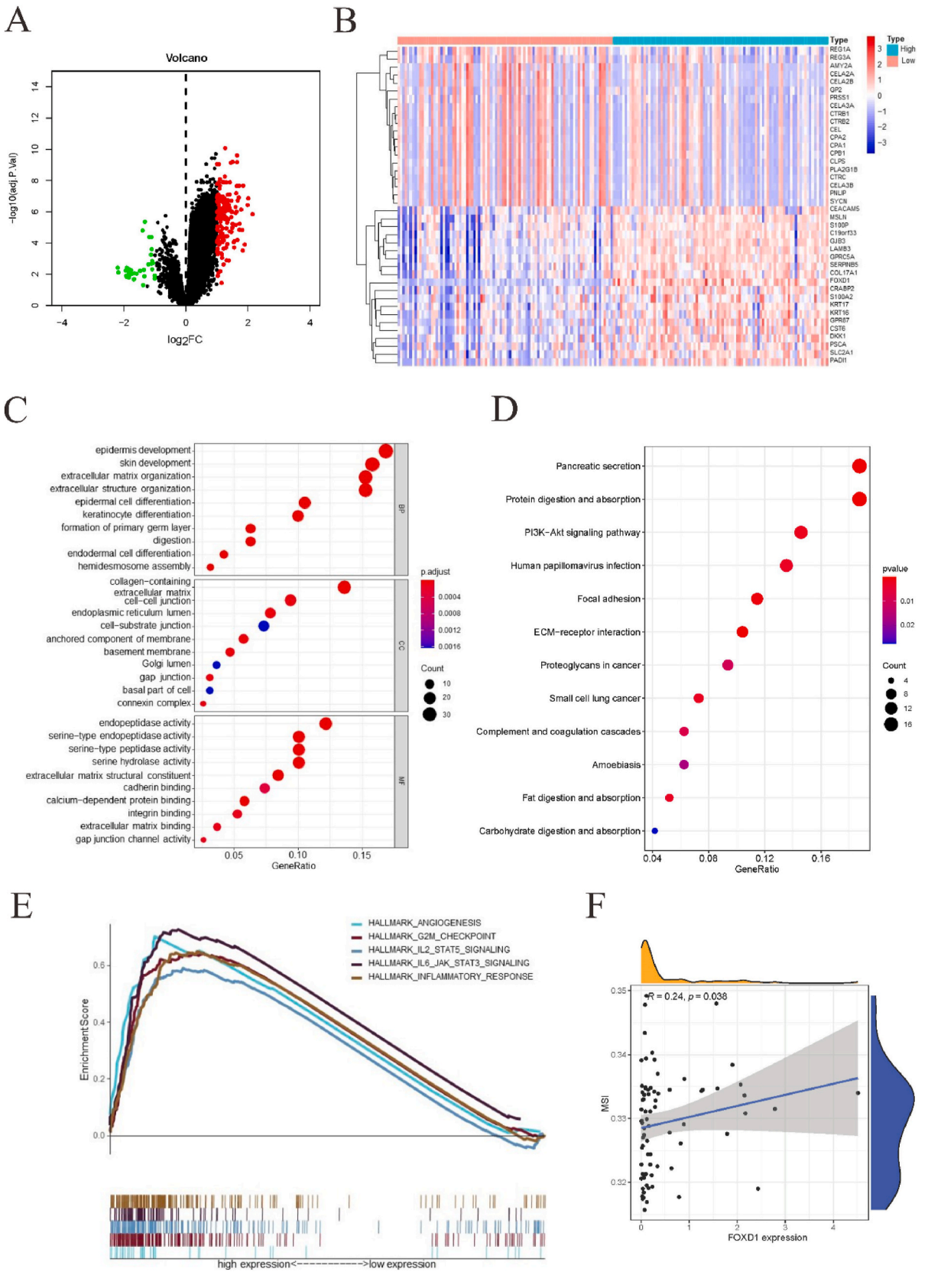

(caption on next page)

Fig. 5. Differential gene expression and function enrichment analysis. **(A, B)** Screening and display of differential genes; **(C)** GO enrichment analysis; **(D)** KEGG enrichment analysis; **(E)** Gene set enrichment analysis; **(F)** Correlation between *FOXD1* and MSI.

3.2. Analysis of the correlation between FOXD1 and UVM prognosis

3.2.1. Analysis of single-nucleotide mutation

High-resolution electrochemical biosensors have been developed for the detection of the four bases in DNA [20]. Genes *GNAQ*, *GNA11*, *BAP1*, *SF3B1*, and *EIF1AX* were once discovered to frequently mutated in UVM patients [21]. Analysis using the R "maftools" package revealed that *GNAQ* and *GNA11* were mutated in patients with high-*FOXD1* and low-*FOXD1* expression. The mutation rate reached 47.4 % and 46.1 %, respectively. Meanwhile, the *BAP1* mutation rate was 28.9 %. Patients with these mutations were mainly concentrated in the group of patients with high-*FOXD1* expression. Whilst, *SF3B1* and *EIF1AX* mutation occurs mainly in patients with low-*FOXD1* expression, accounting for 19.7 % and 13.2 % of the total number of patients, respectively (Fig. 4).

3.2.2. Functional enrichment analysis of DEGs

DEGs between patients with high- and low-*FOXD1* expression were screened out in order to analyze the biological functions and molecular pathways of *FOXD1*-related genes (Fig. 5A and B). GO analysis demonstrated that these genes are mainly involved in: "epidermis development", "skin development", "extracellular matrix organization", and "extracellular structure organization" in Biological Process (BP); "collagen-containing extracellular matrix" and "cell-cell junction" in Cellular Component (CC); "endopeptidase activity", "serine-type endopeptidase activity", "serine-type peptidase activity", and "serine hydrolase activity" in Molecular Function (MF) (Fig. 5C). KEGG analysis revealed that these genes are mainly enriched in the regulation of pathways such as "pancreatic secretion", "protein digestion and absorption", "*PI3K-Akt* signaling pathway", "Human papillomavirus infection", and "Focal adhesion" (Fig. 5D). GSEA revealed that the pathways involved in: "angiogenesis", "*G2M*-checkpoint", "*IL2-stat5*-signaling", "*IL6-jak-stat3*-signaling" and "inflammatory response" were up-regulated by high-*FOXD1* expression in UVM (Fig. 5E). These results indicated that *FOXD1* may regulates tumor growth, metabolism, and inflammatory microenvironment.

3.2.3. Correlation of FOXD1 expression with MSI

MSI is an important marker of DNA mismatch repair defects in tumor tissues [22]. Analysis of 80 UVM patients revealed that the MSI score increased with the increase of *FOXD1* expression level, and the correlation between them was statistically significant ($p = 0.038$, Fig. 5F). That is, MSI was positively correlated with *FOXD1* expression, indicating that *FOXD1* induces DNA mismatch repair defects.

3.2.4. FOXD1 expression and immune cells infiltration

To examine the correlation of *FOXD1* expression with the tumor microenvironment, the proportion and activation of infiltrating immune cells were examined. The immune cells were filtered ($p < 0.05$) to display the proportion of 22 types of infiltrating immune cells into 37 UVM patients (Fig. 6A). *FOXD1* was positively correlated with the proportion of "dendritic cells resting" and "T cells CD4 memory activated"; negatively correlated with the proportion of "plasma cells" and "monocytes" (Fig. 6B). ssGSEA showed that the scores for most of immune-related pathways and immune cells were higher in *FOXD1* high-expression group (Fig. 6C). This result indicates that immune-related pathways and immune cells were more activated in patients with high *FOXD1* expression than low-expression patients.

3.2.5. FOXD1 contributes to immune evasion and drug resistance in tumors

This study examined the sensitivity of tumors to immunotherapy by analyzing the expression of immune checkpoints. Immune checkpoint gene expression was represented as box diagrams (Fig. S2A). The immune checkpoint expression level, including the well-known immune checkpoints like CTLA4 and PDCD1, in the high-*FOXD1* expression patients was higher than that in the low-*FOXD1* expression patients. Overexpression of immune checkpoint molecules promotes the exhaustion of antitumor T cells and enables tumor cells to escape the immune surveillance of the host. Immune evasion of tumors was evaluated using TIDE. The TIDE score is directly proportional to the probability of escape from immune surveillance but inversely proportional to the success rate of immunotherapy. In this study, patients with high-*FOXD1* expression have a higher TIDE score than patients with low-*FOXD1* (Fig. S2B). These results indicate that *FOXD1* promotes immune evasion of tumors and decreases immunotherapy efficacy.

Among the chemotherapy drugs, DNA synthesis inhibitors and tyrosine kinase inhibitors are reported to be potential clinical therapeutics for UVM [23,24]. This study selected cytarabine, bleomycin, axitinib, bosutinib and sunitinib to test the sensitivity to the drugs for the two groups of patients, respectively. The results showed that patients with high-*FOXD1* expression have a higher IC50 scores than patients with low-*FOXD1*. Thus, the patients with high-*FOXD1* expression were less sensitive to these five drugs than those with low-*FOXD1*(Figs. S2C–G).

3.3. Establishment of a prognostic model based on FOXD1-related immune regulatory genes

3.3.1. Construction and evaluation of risk-score models

The immuno-inhibitors and immune-stimulants significantly associated with *FOXD1* expression were screened (Figs. S3 and S4). Univariate Cox regression analysis showed that *TMEM173*, *TNFRSF4*, *TNFSF13*, and *ULBP1* were significantly correlated with *FOXD1*

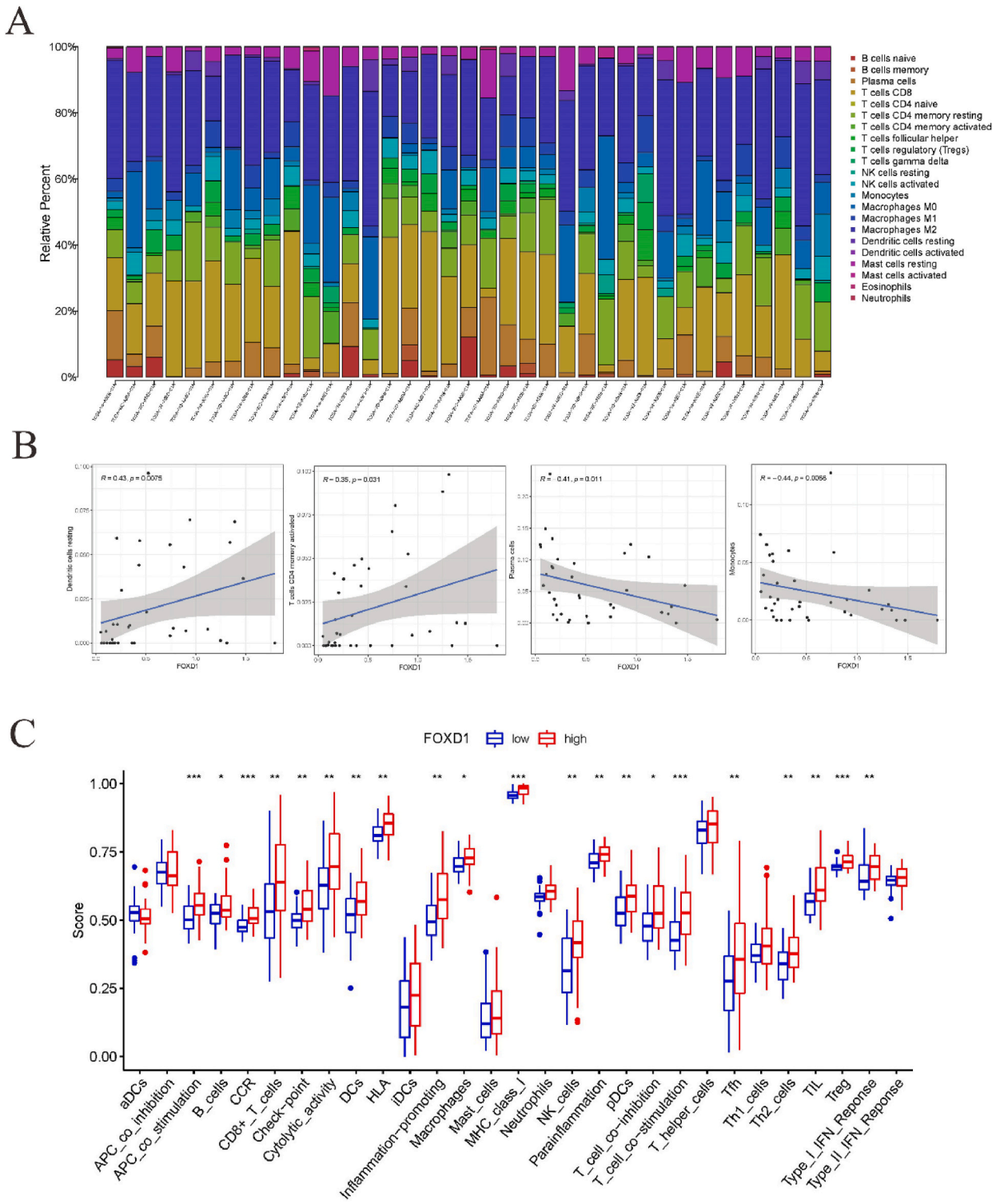

Fig. 6. *FOXD1* expression and immune cells infiltration. **(A)** The infiltration ratio of 22 immune cells in patients; **(B)** Correlation between *FOXD1* and immune infiltrating cells; **(C)** ssGSEA examined the activities of 13 immune-related pathways and infiltration score of 16 immune cells. $P < 0.05$ considered as statistically significance, $^{*}p < 0.05$, $^{**}p < 0.01$, $^{***}p < 0.001$.

(Fig. 7A). A risk score model was constructed using the LASSO method (Fig. 7B). UVM patients were separated into high-risk and low-risk groups according to the best risk-score cutoff. *TMEM173, TNFRSF4,* and *ULBP1* were found to mainly express in high-risk patients,

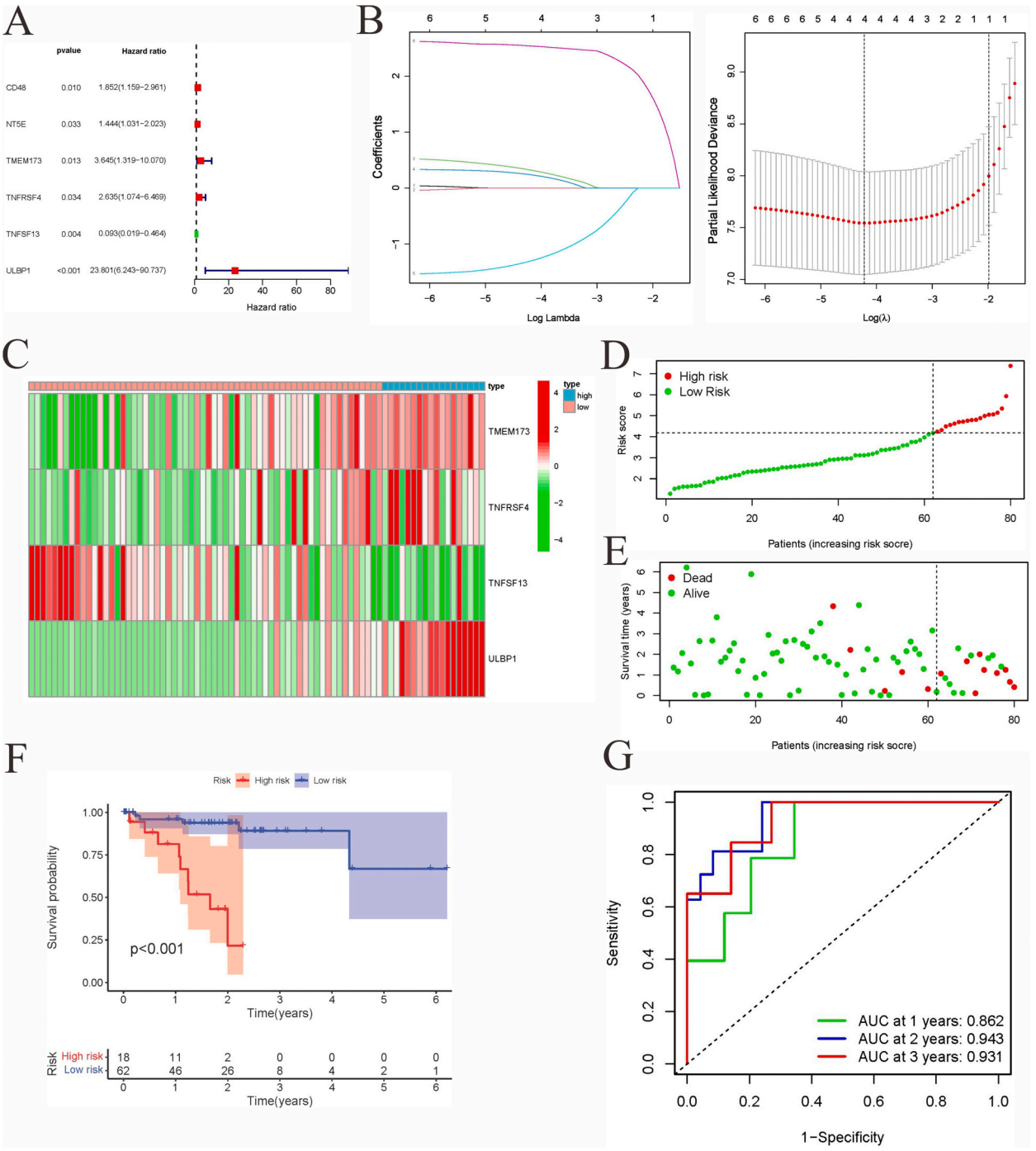

Fig. 7. Construction and evaluation of prognostic models. **(A)** Univariate Cox regression analysis of immunomodulators; **(B)** Removing redundant immunomodulators based on LASSO method; **(C–E)** Expression of *FOXD1*-related immunomodulators, Risk score and survival status in high-risk and low-risk groups; **(F)** Overall survival analysis in high-risk and low-risk groups; **(G)** ROC analyses of 1-, 2- and 3-years overall survival.

while *TNFSF13* mainly expressed in low-risk patients (Fig. 7C, red). The risk scores of 80 patients were displayed in Fig. 7D. Most deaths were recorded in high-risk patients (Fig. 7E). The analyses of patient survival showed that the OS of low-risk patients was higher than that of high-risk patients (Fig. 7F). The AUC values were 0.862, 0.943 and 0.931 for predicting 1-, 2- and 3-years OS, respectively, indicating that the risk-score model had an accuracy in predicting the OS of UVM patients, as shown in Fig. 7G.

3.3.2. *Validation of risk-score models with external queue*

To validate the risk-score model, the data of 28 UVM patients from GSE84976 dataset in GEO database were used as external queue. Similarly, UVM patients are divided into high-risk (5 patients) and low-risk (23 patients) groups. Genes *TMEM173, TNFRSF4,* and *ULBP1* were found to mainly express in high-risk patients; whilegene*TNFSF13*mainly expressed in low-risk patients (Fig. 8A, red). The risk scores of 28 patients were displayed in Fig. 8B. It is worth mentioning that 5 patients with high-risk scores died during the tracking period (Fig. 8C). Survival analyses revealed that the OS of low-risk patients was higher than that of high-risk patients. The 10-year survival rate of the low-risk patients was approximately 17.39 % (Fig. 8D). The AUC value was 0.567 for predicting 3-years OS, indicating that the risk-score model had a certain accuracy in predicting the OS in UVM patients from GSE84976 dataset (Fig. 8E). Thus, the establishment of this risk score model was reasonable.

3.3.3. *Construction and evaluation of self-made nomogram*

The risk-score, gender and TNM stage were evaluated via univariate and multivariate Cox regression analyses (Fig. 9A and B). The results indicated that the risk-score is a reliable indicator for predicting the seriousness of UVM patients. On the basis, A nomogram was constructed by combining the risk score, gender, and TNM stage (Fig. 9C). The AUC values were 0.979, 0.957 and 0.931 for predicting OS of 1-, 3- and 5-years, respectively, indicating that the nomogram model had an accuracy in predicting the OS in UVM patients (Fig. 9D). The construction of the clinical nomogram will provide a theoretical basis for evaluating the long-term survival of patients

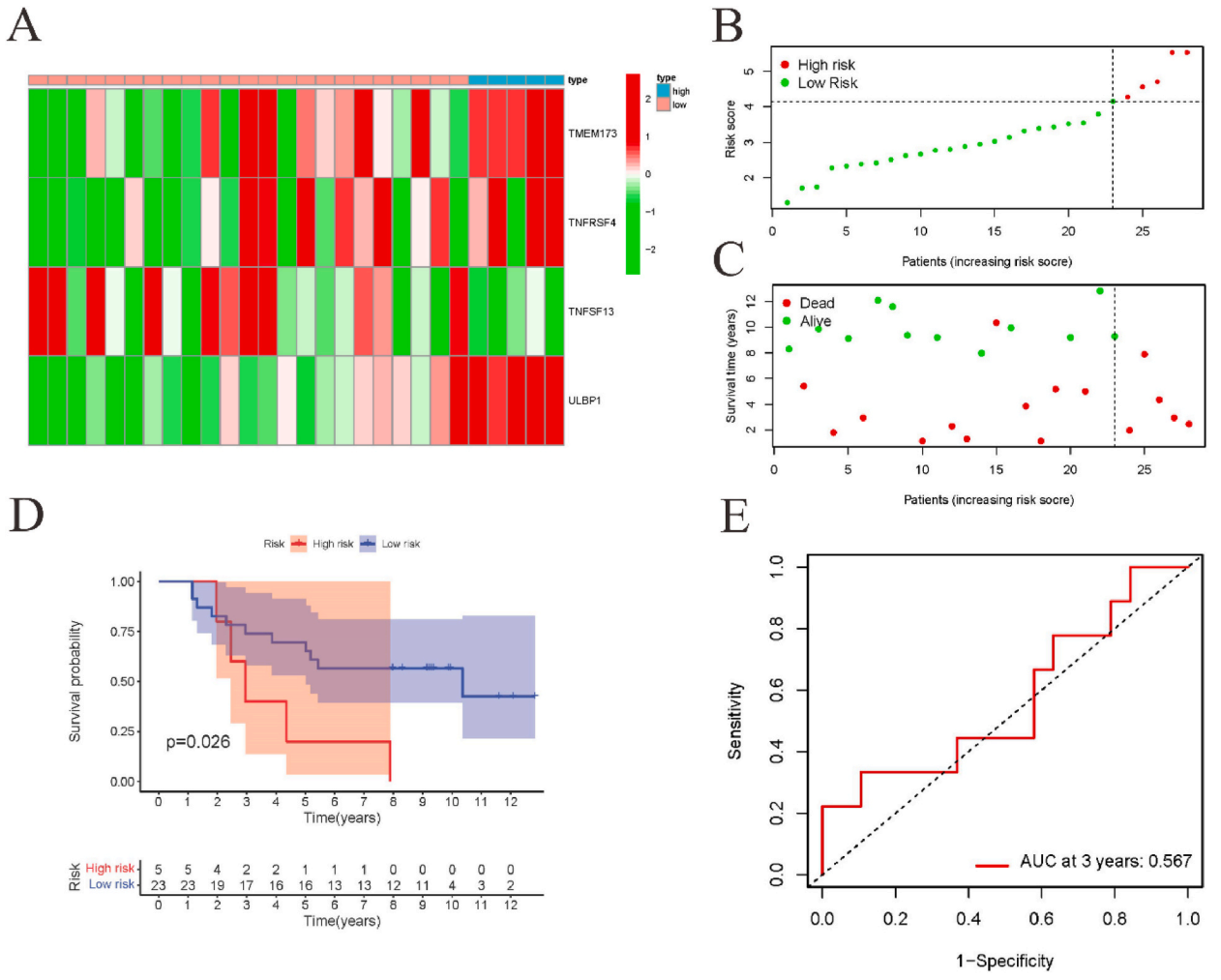

Fig. 8. Verification of prognostic models. **(A–C)** Expression of *FOXD1*-related immunomodulators, Risk score and survival status in high-risk and low-risk groups; **(D)** Overall survival analysis in high-risk and low-risk groups; **(E)** ROC analyses of 3-years overall survival.

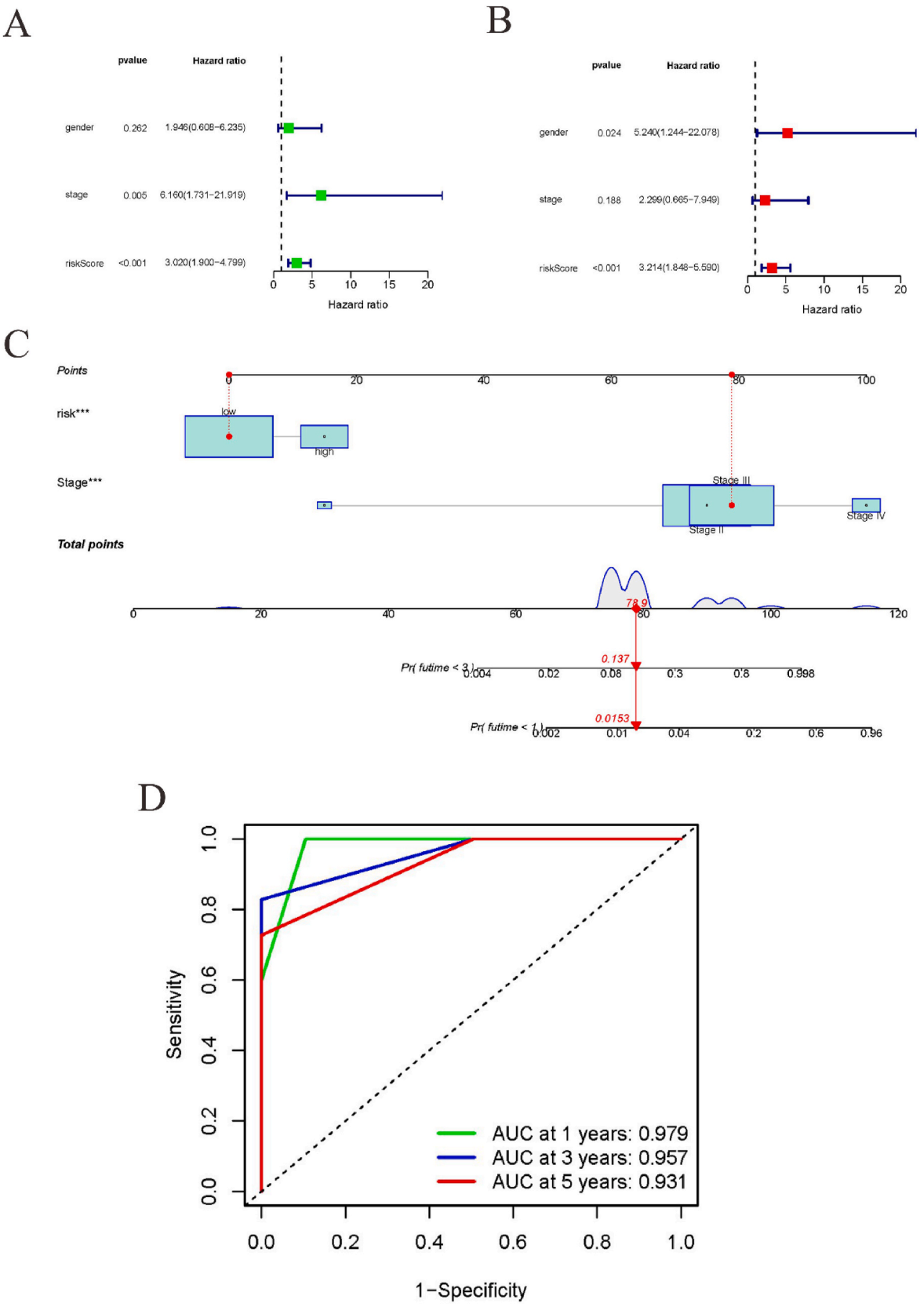

(caption on next page)

Fig. 9. Construction and evaluation of clinical nomogram. **(A, B)** Risk-score, gender and TNM stage were integrated and evaluated via univariate and multivariate Cox regression analyses; **(C)** The nomogram for predicting 1- and 3-years overall survival; **(D)** ROC analyses of the nomogram predicting of 1-, 3- and 5-years overall survival.

and a reference value for the diagnosis and treatment of UVM.

4. Discussion

UVM, a common malignant tumor of the eyes, often leads to the death of patients. *FOXD1*, a member of the *FOX* transcription factor family, is associated with the progression of various tumors [14–19]. However, the correlation between *FOXD1* and the prognosis of UVM has not been elaborated in detail so far. The present work analyzed the correlation between *FOXD1* and the progression of UVM, and established a prognostic model based on *FOXD1*-related immune regulatory genes.

We found that OS, PFS and DSS of the low-*FOXD1* expression patients were significantly higher than those in high-*FOXD1* ones. As the survival of patients is dependent on the progression of UVM, the expression of *FOXD1* was hypothesized to accelerate UVM progression. To validate this hypothesis, cultured MUM2B cells were used as a model. Lentivirus-mediated *FOXD1* knockdown decreased the proliferation and migration of UVM cells. This suggests that *FOXD1* could be a target for UVM treatment. Previous studies [25] have reported that *FOXD1* promotes epithelial-mesenchymal transition and cell stemness in oral squamous carcinoma through the transcriptional activation of *SNAI2*. The upregulation of *FOXD1* promotes the oncogenic transformation through activating vimentin in non-small cell lung cancer [26]. These results suggest that *FOXD1* may promotes the progression of several tumors.

Subsequently, we analyzed the *FOXD1*-related genomic spectrum, molecular pathways, tumor microenvironment and drug treatment sensitivity to further understand the potential role of *FOXD1* in UVM. *GNAQ* and *GNA11* mutations are reported to promote UVM oncogenesis, while *BAP1*, *SF3B1*, or *EIF1AX* mutations are predictors of metastasis [27]. In this study, patients with both high-*FOXD1* and low-*FOXD1* expression had got the mutations in *GNAQ* and *GNA11* genes, which are consistent with the findings of previous studies [27]. *BAP1* mutation mainly occurred in patients with high-*FOXD1* expression, while *SF3B1* and *EIF1AX* mutations were frequent in patients with low-*FOXD1* expression. *BAP1* mutations increase the risk of UVM metastasis and contribute to poor prognosis, while *EIF1AX* mutations are often associated with good prognosis. *SF3B1* mutations are associated with advanced metastasis of tumors. The metastasis risk with *SF3B1* mutations is lower than that with *BAP1* mutations [28–30]. Based on these results, *FOXD1* was speculated to be correlated with *BAP1* mutations. Although this correlation is not clear, the upregulation of *FOXD1* increases the risk of UVM metastasis, which may be one of the reasons for poor prognosis of UVM patients. Van et al. reported similar results [31].

The signaling pathways and biological functions in which *FOXD1* and related genes were enriched were determined. The enriched "*PI3K-Akt* signaling pathway" plays a role in promoting tumor migration and invasion in UVM [32]. GSEA revealed that *FOXD1* upregulated "angiogenesis", "*G2M*-checkpoint", "*IL2-stat5*-signaling", "*IL6-jak-stat3*-signaling" and "inflammatory response". Cancer cells are more rely on G2 checkpoint for DNA damage repair than healthy cells. The activation of "G2M checkpoint" decreases the sensitivity of cancer cells to DNA-damaging drugs and maintains survival [33]. More interestingly, *FOXD1* expression is associated with DNA mismatch repair defects, suppressing the effective clearance of mutant cells and promoting cancer occurrence. The activation of the "angiogenesis," "*IL2-STAT5*-signaling," "*IL6-JAK-STAT3*-signaling," and "inflammatory response" pathways adversely affected the inflammatory tumor microenvironment and consequently increased the malignancy of tumors [9,34].

The density of infiltrating immune cells in tumors represents the efficiency of antitumor immune response. However, this is not observed in patients with UVM. Zhao et al. reported that upregulated infiltration of immune cells contributes to the poor prognosis in UVM patients [35]. In our study, *FOXD1* was positively correlated with the proportion of "dendritic cells (resting)" and "T cells (CD4 memory activated)", indicating that the aberrant expression of *FOXD1* reduces the immune activity of the body by suppressing the infiltration of tumor immune cells, which leads to poor prognosis. The results of ssGSEA displayed that immune-related pathways and immune cells were more activated in the high-*FOXD1* expression patients than those of low expression, including CD8 T cells, NK cells, macrophages and Treg, etc. The enhanced infiltration of these immunocytes cannot enhance the immune capacity of the body, but can accelerate the progression of UVM, which was also recognized by the literature reported [36].

The activation of immune checkpoints enables tumor cells to escape immune surveillance of the host. In our results, immune checkpoints such as *CTLA4* and *PDCD1* were highly expressed in the high-*FOXD1* expression patients, indicating that *FOXD1* promotes tumor immune evasion. This result is consistent with that of TIDE analysis. These findings can explain the poor clinical efficacy of immunotherapy in the high-*FOXD1* expression group. The upregulation of *FOXD1* also decreased the sensitivity of UVM patients to some chemotherapeutic drugs, which may be related to the aberrant activation of the "G2M checkpoint."

FOXD1 is associated with some gene mutations and modulates the tumor microenvironment and drug sensitivity, which let the patients get poor prognosis of UVM. Further, the potential of *FOXD1*-associated immunomodulator-encoding genes to establish a robust model, complement the prediction of the traditional TNM stage system, and guide clinical treatment in the future was evaluated. *FOXD1*-related immunomodulators were retrieved from TISIDB website, in which four immunomodulators, *TMEM173*, *TNFRSF4*, *TNFSF13*and *ULBP1*, were screened by univariate Cox and LASSO regression analysis. *TMEM173* encodes the protein STING (stimulator of interferon gene), which mediates the host defense response against pathogens [37]. However, the TMEM173/STING-dependent DNA sensor pathway promotes pancreatic tumorigenesis [38]. *TNFRSF4* is a marker for poor prognosis in acute myeloid leukemia [39], while *TNFSF13* functions as a positive regulator of leukemia-initiating cells [40]. The upregulation of *TNFSF13* is related to the progression of various tumors like glioma [41] and breast tumors [42], However, *TNFSF13* derived from

activin A-treated dendritic cells can enhance the antitumor effect of dendritic cells [43]. *ULBP1*, a member of the ligand family of natural killer Cell Group 2 receptor D (*NKG2D*), is closely related to the prognosis of tumors. Patients with high-*ULBP1* expression had significantly longer survival time than patients with low-*ULBP1* in cervical cancer [44]. However, the aberrant upregulation of *ULBP1* increased the death risk of colon adenocarcinoma patients and promoted the immune escape in hepatocellular carcinoma [45,46].

In this study, *TMEM173, TNFRSF4, TNFSF13* and *ULBP1* were employed to setup a risk assessment model. The accuracy of this model was verified using the data from the external database. Through univariate and multivariate Cox regression analyses, we confirmed that the risk-score is a reliable indicator for predicting the seriousness of UVM patients. Next, a novel nomogram was established by combining the risk-score with the clinical variables gender and TNM stage. This nomogram may provide a theoretical basis for evaluating the long-term survival of patients and a reference value for patient diagnosis and treatment of UVM.

In summary, this study demonstrated the correlation between *FOXD1* and UVM prognosis. Additionally, a novel prognostic model for UVM was established, which will enable the stratification of disease severity and the effective clinical treatment of patients. We hope that gene therapy will be developed for UVM that carries such a poor prognosis.

Ethics approval and consent to participate

Not applicable.

Consent for publication

All authors give their consent to publish this manuscript.

Data availability statement

Data will be made available on request.

Funding

This work was supported by Basic Public Welfare Research Program of Zhejiang Province (LY21H120001).

CRediT authorship contribution statement

Yang Luo: Data curation, Formal analysis, Writing – original draft, Project administration. **Renhao Ni:** Data curation, Formal analysis. **Xiaojun Jin:** Data curation, Formal analysis. **Peipei Feng:** Data curation, Formal analysis. **Chenyi Dai:** Data curation, Formal analysis. **Lingjing Jiang:** Data curation, Formal analysis. **Pingping Chen:** Data curation, Formal analysis. **Lu Yang:** Funding acquisition, Project administration, Validation, Writing – review & editing. **Yabin Zhu:** Project administration, Validation, Writing – review & editing.

Declaration of competing interest

The authors declare that they have no known competing financial interests or personal relationships that could have appeared to influence the work reported in this paper.

Acknowledgements

We are grateful to OE Biotech, Inc., (Shanghai, China) for assisting in sequencing.

Appendix A. Supplementary data

Supplementary data to this article can be found online at https://doi.org/10.1016/j.heliyon.2023.e21333.

References

[1] S. Kaliki, C.L. Shields, Uveal melanoma: relatively rare but deadly cancer, Eye (London, England) 31 (2) (2017) 241–257.
[2] C. Chattopadhyay, et al., Uveal melanoma: from diagnosis to treatment and the science in between, Cancer 122 (15) (2016) 2299–2312.
[3] S. Kaliki, C.L. Shields, J.A. Shields, Uveal melanoma: estimating prognosis, Indian J. Ophthalmol. 63 (2) (2015) 93–102.
[4] E.B. Souto, et al., Uveal melanoma: physiopathology and new in situ-specific therapies, Cancer Chemother. Pharmacol. 84 (1) (2019) 15–32.
[5] J.W. Harbour, et al., Frequent mutation of BAP1 in metastasizing uveal melanomas, Science 330 (6009) (2010) 1410–1413.
[6] M.G. Field, J.W. Harbour, Recent developments in prognostic and predictive testing in uveal melanoma, Curr. Opin. Ophthalmol. 25 (3) (2014) 234–239.
[7] S. Landreville, et al., Histone deacetylase inhibitors induce growth arrest and differentiation in uveal melanoma, Clin. Cancer Res. 18 (2) (2012) 408–416.
[8] B. Arneth, Tumor microenvironment, Medicina (Kaunas) 56 (1) (2019).

[9] I.H. Bronkhorst, M.J. Jager, Uveal melanoma: the inflammatory microenvironment, J. Innate Immun. 4 (2012) 454–462.
[10] L.A. Kottschade, et al., The use of pembrolizumab for the treatment of metastatic uveal melanoma, Melanoma Res. 26 (3) (2016) 300–303.
[11] J. Huang, B. Liang, T. Wang, FOXD1 expression in head and neck squamous carcinoma: a study based on TCGA, GEO and meta-analysis, Biosci. Rep. 41 (7) (2021).
[12] P. Quintero-Ronderos, P. Laissue, The multisystemic functions of FOXD1 in development and disease, J. Mol. Med. 96 (8) (2018) 725–739.
[13] M. Koga, et al., Foxd1 is a mediator and indicator of the cell reprogramming process, Nat. Commun. 5 (2014) 3197.
[14] Y. Ma, J. Han, X. Luo, FOXD1-AS1 Upregulates FOXD1 to Promote Oral Squamous Cell Carcinoma Progression, Oral diseases, 2021.
[15] H. Liang, et al., FOXD1 is a prognostic biomarker and correlated with macrophages infiltration in head and neck squamous cell carcinoma, Biosci. Rep. 41 (7) (2021).
[16] Q. Wu, et al., FOXD1-AS1 regulates FOXD1 translation and promotes gastric cancer progression and chemoresistance by activating the PI3K/AKT/mTOR pathway, Mol. Oncol. 15 (1) (2021) 299–316.
[17] C.H. Li, et al., FOXD1 and gal-3 form a positive regulatory loop to regulate lung cancer aggressiveness, Cancers 11 (12) (2019).
[18] C. Chen, et al., CXCL5 induces tumor angiogenesis via enhancing the expression of FOXD1 mediated by the AKT/NF-κB pathway in colorectal cancer, Cell Death Dis. 10 (3) (2019) 178.
[19] K.H. Bond, et al., FOXD1 regulates cell division in clear cell renal cell carcinoma, BMC Cancer 21 (1) (2021) 312.
[20] O. Akhavan, E. Ghaderi, R. Rahighi, Toward single-DNA electrochemical biosensing by graphene nanowalls, ACS Nano 6 (4) (2012) 2904–2916.
[21] M. Dono, et al., Mutation frequencies of GNAQ, GNA11, BAP1, SF3B1, EIF1AX and TERT in uveal melanoma: detection of an activating mutation in the TERT gene promoter in a single case of uveal melanoma, Br. J. Cancer 110 (4) (2014) 1058–1065.
[22] E. Vilar, S.B. Gruber, Microsatellite instability in colorectal cancer-the stable evidence, Nat. Rev. Clin. Oncol. 7 (3) (2010) 153–162.
[23] A. Mahipal, et al., A pilot study of sunitinib malate in patients with metastatic uveal melanoma, Melanoma Res. 22 (6) (2012) 440–446.
[24] C. Pföhler, et al., Treosulfan and gemcitabine in metastatic uveal melanoma patients: results of a multicenter feasibility study, Anti Cancer Drugs 14 (5) (2003) 337–340.
[25] Y. Chen, et al., FOXD1 promotes EMT and cell stemness of oral squamous cell carcinoma by transcriptional activation of SNAI2, Cell Biosci. 11 (1) (2021) 154.
[26] D. Li, et al., FOXD1 promotes cell growth and metastasis by activation of vimentin in NSCLC, Cell. Physiol. Biochem. : international journal of experimental cellular physiology, biochemistry, and pharmacology 51 (6) (2018) 2716–2731.
[27] K.N. Smit, et al., Uveal melanoma: towards a molecular understanding, Prog. Retin. Eye Res. 75 (2020), 100800.
[28] J.J. Park, et al., Oncogenic signaling in uveal melanoma, Pigment Cell Melanoma Res 31 (6) (2018) 661–672.
[29] S. Yavuzyigitoglu, et al., Uveal melanomas with SF3B1 mutations: a distinct subclass associated with late-onset metastases, Ophthalmology 123 (5) (2016) 1118–1128.
[30] B. Masoomian, J.A. Shields, C.L. Shields, Overview of BAP1 cancer predisposition syndrome and the relationship to uveal melanoma, Journal of current ophthalmology 30 (2) (2018) 102–109.
[31] Q.C.C. van den Bosch, et al., FOXD1 is a transcription factor important for uveal melanocyte development and associated with high-risk uveal melanoma, Cancers 14 (15) (2022).
[32] M. Farhan, et al., Artemisinin inhibits the migration and invasion in uveal melanoma via inhibition of the PI3K/AKT/mTOR signaling pathway, Oxid. Med. Cell. Longev. 2021 (2021), 9911537.
[33] N. Bucher, C.D. Britten, G2 checkpoint abrogation and checkpoint kinase-1 targeting in the treatment of cancer, Br. J. Cancer 98 (3) (2008) 523–528.
[34] I.H. Bronkhorst, M.J. Jager, Inflammation in uveal melanoma, Eye (London, England) 27 (2) (2013) 217–223.
[35] H. Zhao, et al., Identification of immune cell infiltration landscape and their prognostic significance in uveal melanoma, Front. Cell Dev. Biol. 9 (2021), 713569.
[36] S. García-Mulero, et al., Additive role of immune system infiltration and angiogenesis in uveal melanoma progression, Int. J. Mol. Sci. 22 (5) (2021).
[37] S. Patel, L. Jin, TMEM173 variants and potential importance to human biology and disease, Genes Immun 20 (1) (2019) 82–89.
[38] E. Dai, et al., Ferroptotic damage promotes pancreatic tumorigenesis through a TMEM173/STING-dependent DNA sensor pathway, Nat. Commun. 11 (1) (2020) 6339.
[39] S. Gu, et al., Elevated TNFRSF4 gene expression is a predictor of poor prognosis in non-M3 acute myeloid leukemia, Cancer Cell Int. 20 (2020) 146.
[40] M. Chapellier, et al., Arrayed molecular barcoding identifies TNFSF13 as a positive regulator of acute myeloid leukemia-initiating cells, Haematologica 104 (10) (2019) 2006–2016.
[41] R. Chen, et al., TNFSF13 is a novel onco-inflammatory marker and correlates with immune infiltration in gliomas, Front. Immunol. 12 (2021), 713757.
[42] A. García-Castro, et al., APRIL promotes breast tumor growth and metastasis and is associated with aggressive basal breast cancer, Carcinogenesis 36 (5) (2015) 574–584.
[43] M.R. Shurin, et al., BAFF and APRIL from activin A-treated dendritic cells upregulate the antitumor efficacy of dendritic cells in vivo, Cancer Res. 76 (17) (2016) 4959–4969.
[44] H. Cho, et al., MICA/B and ULBP1 NKG2D ligands are independent predictors of good prognosis in cervical cancer, BMC Cancer 14 (2014) 957.
[45] G.T. Ruan, et al., Immune ULBP1 is elevated in colon adenocarcinoma and predicts prognosis, Front. Genet. 13 (2022), 762514.
[46] F. Qi, et al., viaTumor mutation burden-associated LINC00638/miR-4732-3p/ULBP1 Axis promotes immune escape PD-L1 in Hepatocellular carcinoma, Front. Oncol. 11 (2021), 729340.